AD-A143 014 T-MOTOR TESTS WITH CYLINDRICAL GRAINS(U) FOREIGN TECHNOLOGY DIV WRIGHT-PATTERSON AFB OH K YEH 16 JUL 84 FTD-ID(RS)T-0779-84 1/1

UNCLASSIFIED F/G 21/8.2 NL

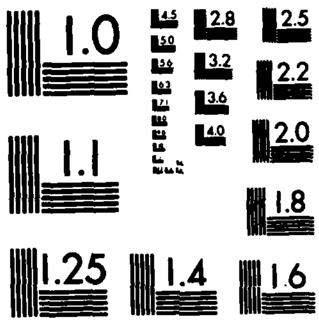

MICROCOPY RESOLUTION TEST CHART
NATIONAL BUREAU OF STANDARDS-1963-A

FTD-ID(RS)T-0779-84

FOREIGN TECHNOLOGY DIVISION

AIR FORCE SYSTEMS COMMAND

T-MOTOR TESTS WITH CYLINDRICAL GRAINS

by

K. Yeh

FOREIGN TECHNOLOGY DIVISION

EDITED TRANSLATION

FTD-ID(RS)T-0779-84 16 July 1984

MICROFICHE NR: FTD-84-C-000708

T-MOTOR TESTS WITH CYLINDRICAL GRAINS

By: K. Yeh

English pages: 7

Source: Gongcheng Rewuli Xuebao, Vol. 4,
Nr. 3, August 1983, pp. 304-306

Country of origin: China
Translated by: SCITRAN
F33657-81-D-0263
Requester: FTD/TQTA
Approved for public release; distribution unlimited.

GRAPHICS DISCLAIMER

All figures, graphics, tables, equations, etc. merged into this translation were extracted from the best quality copy available.

T-MOTOR TESTS WITH CYLINDRICAL GRAINS* /304***

Kao Yeh** (The Peiching Institute Of Technology)

ABSTRACT

In this paper, some experimental results have been given for T-motor tests with cylindrical grains. These show that, within a certain boundary of grain geometry, the response function is independent of the combustion surface area of the propellant.

I. Experimental Conditions and Characteristics of Cylindrical Grains

The combustion chamber used in the experiment has an inner diameter of 5 cm, and inner length of 50 cm. As changes in the combustion surface area produce variations in pressure, the latter can be controlled to lie within the required range by switching to different combustion chamber nozzles with various throat diameters. The BYY-3 transducer for measuring the static pressure and the BPR-3 transducer for measuring the oscillatory pressure are installed separately at the two ends of the combustion chamber. One end of the cylindrical grains is glued to the compressed choke head of the combustion chamber by means of an epoxy resin mixture, and the other end is wrapped in cloths treated with a nitrate-based paint to ensure even surface combustion. The initial temperature of the grains is kept within the temperature range of 10-25 °C, and the equilibrium pressure of the acoustic energy growth section is controlled to lie between 50 and 80 kg/cm^2. A double-lead-2 solid propellant is used in the experiment, and

---

*This paper was read in October of 1982 at the Third Annual Chinese Engineering Thermophysics Conference held in Wuhsi.

**This work has been completed under the guidance of Prof. P'eng Choayuen.

***Numbers in margin indicate foreign pagination black gunpowder is used for ignition. As the combustion surface area increases from 65 cm^2 to 228.6 cm^2, the amount of ignition gun powder used is increased accordingly. A typical experimental curve as recorded on a SC-18 oscilloscope is shown in Fig. 1.

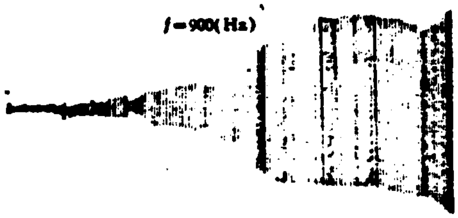

Fig. 1. A typical acoustic vibration growth curve

Using cylindrical grains in T-motors does away with the disadvantage of relatively large damping of end-surface grains, and that of generating residual propellant in annular grains. As the cylindrical grains have sufficient combustion surface area to create a great tendency for acoustic vibrations, the effect of the acoustic damping a_d on the actual value of the acoustic energy growth rate $a = a_g + |a_d|$, which produces a relatively large error in the measurement, becomes correspondingly small.

II. Experimental Results and Analysis

The acoustic energy growth rate of the cylindrical grains can be expressed as:

$$a = \frac{4\gamma R L f}{E_l^2} C_l [A_b + \bar{M}_b] \frac{S_{bl}}{S_{c0}}$$

where

$$A_b = \frac{\hat{u}_b / a_0}{\hat{p}_l / \gamma p_0} \quad \bar{M}_b = \frac{\bar{u}_b}{a_0} \quad C_l = \frac{1}{S_{bl}} \int_0^L \hat{p}_l^2 \int dq\,dx \quad E_l^2 = \frac{1}{2} \int_0^L \hat{p}_l^2 S_c dx \,.$$

Given the gas constant R, specific heat ratio γ, the inner length L of the combustion chamber, the measured frequency f, acoustical energy growth rate α, and the C_1 and ε_ℓ^2 under the given experimental conditions, one can calculate the value for $A_b + \overline{M}_b$. The major divisions of the combustion chamber and the vibration modes of pressure are as shown in Fig. 2. In the diagram, $S_c = S_{c1} + S_{c2}$. Making use of the continuity requirement on the wave motion and mass flow perturbation of the pressure at the radial position $x = x_b$, and introducing the dimensionless quantities $\beta = 2x_b/L$ and $K_1 = L\omega_1/2a_0$, one can obtain the mathematical expressions for computing K_1 and the pressure acoustic vibration modes $\hat{p}_1$

/305

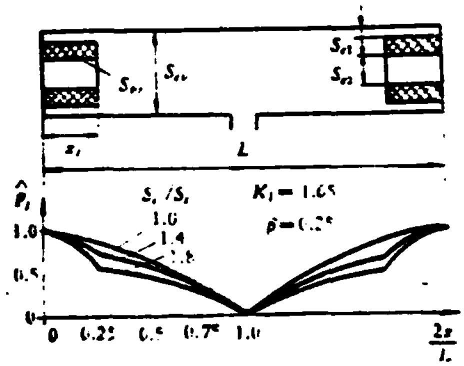

Fig 2. Simplified diagram of the combustion chamber and the acoustic vibration modes

$$(S_{c0}/S_c)\cos K_l(1-\beta) = \mathrm{tg}\, K_l\beta$$

$$\hat{p}_l = \cos K_l 2x/L \quad (当\ 0 \leqslant 2x/L < \beta)$$

$$\hat{p}_l = \frac{S_c/S_{c0}}{\cos K_l(1-\beta)}\sin K_l(1-2x/L)$$

$$(当\ \beta < 2x/L \leqslant 1)$$

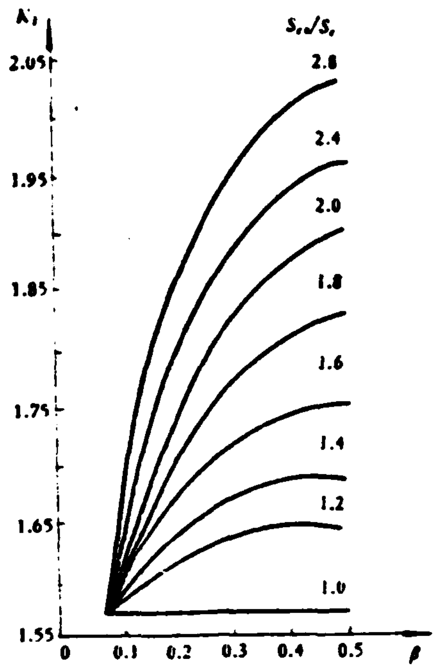

Fig. 3. Relation between the dimensionless frequency and the grain geometry

Fig. 3 shows the variation of K_1 with the area of the combustion chamber passage and grain length. With respect to the present experiment, when the grain geometry is given by D/d——L_b = $38/14$——30, (S_{c0}/S_c = 2.10, β = 0.12), one obtains from Fig. 3 $K_1 = 1.64$. For the double-lead-2 propellant, γ = 1.21, R = 31.67, T_0 = 2500K. Therefore a_0 = $\sqrt{\gamma g R T_0}$ = 968 m/s, $f = K_1 a_0/\pi L$ = 1012 Hz. Owing to heat loss and other damping factors, the actual measured frequencies lie within the range of 890-950 Hz.

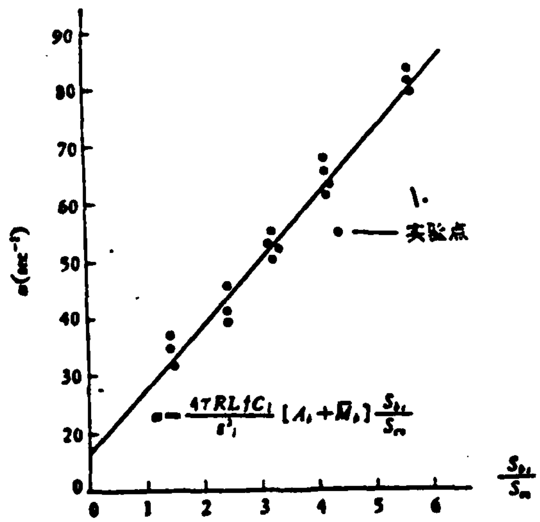

Fig. 4. Relation between acoustic energy growth rate and combustion surface area ratio

1. Experimental points

Knowing how K_1 and $\hat{p}_1$ vary, one can compute the magnitude of C_1 and ε_ℓ^2 with respect to a specific combustion chamber structure. The variation of the experimentally measured acoustic energy growth rate with the combustion surface area ratio is shown in Fig. 4. Price's method has been adopted in the data analysis. It can be seen from the experiment that the linearity and repeatability of the curves for the acoustic attenuation section are far from being ideal. Undoubtedly, variation on the geometrical shape of the propellant and the flow of the mean flow produce a difference between the acoustic vibrational damping combination and that at the completion of the combustion. Fig. 5 shows the acoustic growth rate measured experimentally for 30, 40 and 50 mm grains, respectively. It can be seen that these characteristic curves possess good linearity and conformity.

When the grain geometry is given by D/d——$L_b = 44/8$——80, there appear regularly harmonics due to velocity coupling and serious distortion of the pressure oscillation due to the /306 relatively high mean flow rate. In the course of the combustion, the area of the gas passage is enlarged, the mean flow rate decreases, and the oscillation curve tends to normal.

There is a critical point above which the oscillation curve will be distorted by velocity coupling and excessive mean flow rate. Satisfactory pressure oscillation curves have been obtained in the experiment by changing the grain geometry from D/d——$L_b = 44/8$——80 to $38/14$——70. This is why the maximum grain length has been taken to be 70 mm for this experiment.

III. Conclusion

Nice linear relations between α, β and S_{bs}/S_{c0} can be obtained for a T-motor with cylindrical grains within certain limits set jointly by S_{bs}/S_{c0} and β. This proves that the pressure response function of the propellant is independent of the combustion surface area. Outside of these limits, the resulting abnormality in the pressure acoustic field due to velocity coupling and high mean flow rate is serious. This places a restriction on the choice of values for S_{bs}/S_{c0} and β for T-motors. As a result, linear relationship between α and S_{bs}/S_{c0} can only be obtained within limited ranges.

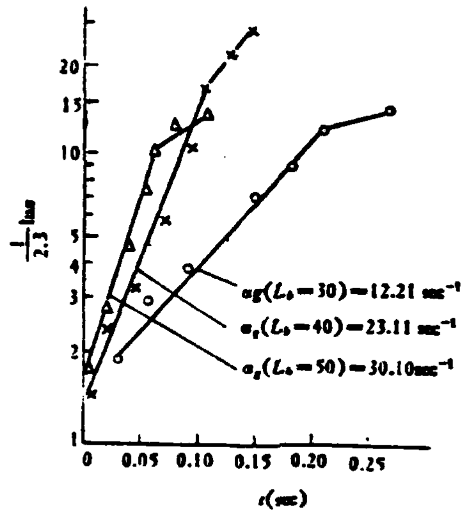

Fig. 5. Linear characteristics of the acoustic energy growth of grains of various lengths

Notations

a_0 stagnation sound velocity

x radial displacement

q circumference of cylindrical grains

D outer diameter (mm) of grains

d innner diameter (mm) of grains

L_b length of grains (mm)

S_{bs} combustion surface area

S_c air passage area

S_{c0} cross-sectional area of combustion chamber

ω_ℓ angular frequency of oscillation

A_b combustion surface sonar

$\hat{p}_t$ complex amplitude of pressure perturbation

$\hat{u}_b$ complex amplitude of the velocity of the gas at the combustion surface

P_0 stagnation pressure

β dimensionless grain length

K_1 dimensionless oscillation frequency

α_g measured acoustic energy growth constant

α_d measured acoustic energy damping constant

T_0 stagnation temperature

z height of sound wave amplitude

References

[1] P'eng Chao-yuan, "Theory and Experiments on Linear Acoustic Oscillation Burning of Solid Propellant Rocket Engines," Lecture Notes, Peiching Institute of Technology, 1979.

[2] F.E.C. Culick, "T-Burner Testing of Metalized Solid Propellants," AD A001665, 1974.

END

FILMED

9-84

DTIC